Urol Res (2012) 40:197–204
DOI 10.1007/s00240-011-0428-0

ORIGINAL PAPER

Characterization of kidney stones using thermogravimetric analysis with electron dispersive spectroscopy

Heow Pueh Lee · Dalun Leong · Chin Tiong Heng

Received: 16 April 2010 / Accepted: 21 September 2011 / Published online: 4 October 2011

Abstract Urinary calculi are formed from a result of biological mal-adjustment of urine leading to deposits of salt and mineral crystals along the urinary collecting system. They are usually multiphasic material with complex compositions. The objective of this study is to identify and characterize a series of urinary calculi samples using a combination of thermogravimetric analysis (TGA) with electron dispersive spectroscopy (EDS). These samples were retrieved during percutaneous nephrolithotripsy. Additional characterization by hardness value and microstructure is also carried out for co-relation study. The samples are found to be uric acid, calcium oxalates and magnesium ammonium phosphate hexahydrate. TGA is indeed one of the viable analytical tools for urinary calculi as it is fast and simple. The combinational application of EDS is beneficial when there is a need for differentiated qualitative chemical composition detection at the identified nuclei position for urinary calculi with spatial variation in composition. The combination of TGA and EDS will thus facilitate the correct diagnosis and treatment by clinicians.

Keywords Urinary calculi · Thermogravimetric analysis · Electron dispersive spectroscopy · Microhardness

H. P. Lee (✉) · D. Leong
Department of Mechanical Engineering, National University of Singapore, 9 Engineering Drive 1, Singapore 117576, Singapore
e-mail: mpeleehp@nus.edu.sg

C. T. Heng
Department of Surgery, National University of Singapore, Singapore, Singapore

C. T. Heng
Urology Department, National University Health System, Singapore, Singapore

Introduction

Urinary calculi are formed from a result of biological mal-adjustment of urine leading to deposits of salt and mineral crystals along the urinary collecting system. The clinical sequelae of urinary stones include acute pain, known as renal or ureteric colic, urinary obstruction leading possibly to damage to kidney function, and infection of an obstructed system, known as pyonephrosis. Urolithiasis or the condition of formation of kidney stones is a fairly common condition, affecting about up to 5% of the industrialized population, with the lifetime risk of passing a kidney stone to be about 8–10% [1]. The current method of choice for the treatment of large kidney stone is percutaneous nephrolithotripsy (PCNL), which fragments the stones via a minimally invasive approach. Fragments about 1 cm or smaller can be removed yielding excellent stone clearance rates. On the other hand, extracorporeal shock-wave lithotripsy (ESWL) is more commonly used for smaller stones, with the resulting sediment and fragments passing naturally down the urinary tract.

Urinary calculi are usually multiphasic materials with complex compositions consisting of multiple mineral constituents. There is therefore a need to conduct both qualitative and quantitative analysis of the samples to establish the chemical composition of the calculus. Once that is done, the stones with relatively similar compositions can be grouped together and their hardness value examined. This hardness value is useful as it largely dictates the manner by which stones react to mechanical stresses induced during ESWL [2]. Therefore, the characterization of urinary calculi is necessary to understand the mechanical properties of such stones, so as to provide suitable treatment parameters during ESWL to minimize the possible side effects. Knowing the composition and microstructure

also helps in correctly diagnosing the causal disease and selecting appropriate treatment modalities [3].

Thermogravimetric analysis (TG or TGA) has been extensively used to analyze kidney stones since the 1970s. Rose and Woodfine [4] advocated the use of TGA for the analysis of stones due to its ability to produce fast and quantitative results. Konjiki et al. [5] coupled TGA with X-ray diffraction, providing a deeper understanding to the mineralogical composition of kidney stones. D'Ascenzo et al. [6] published a study on renal calculi using thermal application of differential thermal analysis (DTA) to reinforce TGA in routine applications. DTA–TG provided a greater ease and accuracy of qualitative analysis due to the signature curves of DTA that accompany each component's decomposition. Materazzi et al. [7] later advocated the simultaneous analysis of TG with Fourier transform infrared (FTIR) spectroscopy. FTIR analyses are simultaneously carried out on the exhaust gas from the decomposition of kidney stones samples arising from the TGA. Based on this approach, the exact material decomposed is known and recorded at each specific temperature. This proved to be an excellent routine method employed by many laboratories today. Ficai et al. [8] presented a study of in vitro characterization of human uroliths using the four methods, namely X-ray diffraction analysis (XRD), scanning electron microscopy (SEM), infrared spectroscopy (IR) using Shimadzu 8400 FTIR Spectrometer and DTA coupled with TGA. The qualitative assignments were based on XRD and FTIR analyses, the morphological investigation were based on SEM, whereas the mass quantification was based on TGA. Another more recently developed method is the combined use of infrared imaging and microanalysis [9]. The reflectance mode of an infrared microscope can be used to create chemically specific maps of cross-sectioned renal calculi surfaces instead of just providing qualitative analysis as reported in the earlier applications.

The internal structure of kidney stones can be differentiated into two groups [2]. The first group contains those that have an obvious laminar structure. The second group consists of those that contain anisotropic distribution of crystalline masses and matrices. The former usually contains either a central or a peripheral nucleus whereas the latter have no visible nuclei. According to D'Ascenzo et al. [6], the nuclei may be chemically composed of different materials compared to the outer shell. For example, the presence of struvite can imply urinary infection. If struvite is present only in the outer layers, it is mostly likely that urinary infection developed as a complication after central nucleus aggregation [10]. If an undifferentiated analysis was to be done, potentially the nuclei constituents might be masked over by the general calculi constituents. This might lead to a misdirected diagnosis. Therefore, in this study where it is appropriate, regional differences will be made known if the qualitative analysis indeed has shown such a distinction. The combination of electron dispersive spectroscopy (EDS) with TGA is introduced in this study so that there is an appreciation of differentiated analysis to the samples.

After the introduction of ESWL in the 1980s, there is an influx of publications trying to improve the ESWL treatments by having a greater understanding of the hardness value of kidney stones. Hardness is defined as the resisting capacity of a material against penetrating loads. Zhong et al. [2, 11] tested the correlation between the hardness and degree of erosion after cavitations exposure and found that it was one of the major factors determining the treatment response during ESWL, along with other factors like ductility and brittleness. They advocated the use of microhardness test as it would provide a simple and convenient method to characterize complex mechanical properties of renal calculi. Conventional hardness test uses a large specimen size, while assuming material homogeneity therefore resulting in a scattered range of hardness values. However, microhardness test allows the repeated measurements of a single sample at different regions, allowing differentiated characterization at different region of a single sample. Cohen and Whitfield [12] proposed that chemical composition was related to stone strength and determined through experimentations that denser and more uniform calculi would be more resistant to ESWL.

The objective of this study is to identify and characterize the urinary calculi (kidney stones) obtained during PCNL for large renal stones (>1.5 cm in longest diameter), using a combination of TGA and EDS. Fragments retrieved via PCNL are larger than those retrieved via ureteroscopy or post-ESWL, allowing an analysis of the macroscopic structure of the stones. Additional characterization by hardness value and microstructure would be done to provide a broader platform for further analyses.

Methods

A total of nine urinary calculi samples were obtained. These were fragmented during surgery using a combination ultrasound and ballistic lithotripter and retrieved percutaneously. These samples ranged in size from 3 to 9 mm in greatest diameter. Routine qualitative chemical analysis showed that they were typical of the stones seen in our practice, viz. chiefly calcium oxalate, uric acid (UA) or magnesium ammonium phosphate stones. The samples were then sterilized and stored in test tubes. A JEOL JSM 5500 scanning electron microscope (SEM) with EDS capability was used for the qualitative analysis of chemical component at specific regions. The SEM was operating on

10 kV with spot size from 25 to 35 nm and the samples are not coated with any materials to improve accuracy of EDS but at the expense of visual clarity. A simultaneous thermal analysis apparatus capable of conducting TG-DTA (Shimadzu DTG-60) was used, with 10–15°C/min heating rate from ambient temperature of 25–900°C under atmospheric condition. Thermocouples, crucibles and thermal inert used were all alumina (Al_2O_3). Each test was characterized by two curves: TG and DTA according to temperature (T in °C). Mass samples were in the range of 15–40 mg. A Shimadzu HMV2 Microhardness Tester was used for the testing of microhardness in distributed regions of the samples. The samples were polished for visual facilitation of the indenters. A diamond indenter was used and loads from 0.4903 to 2.942 N were applied to test the samples. The hardness value was expressed as $HV = 1{,}854\ P/d^2$ where HV was in kg/mm^2 and d is the average diagonal length of a Vickers indentation in mm. P is the load (kg).

EDS is an analytical technique used for elemental analysis or chemical composition of samples [13]. During SEM, the interaction of the primary beam with atoms in the sample may cause shell transitions which results in X-ray emission. The emitted X-ray has energy characteristic of the sample element. EDS therefore can provide rapid qualitative analysis of elemental composition with a sampling depth of 1–2 μm. However, the EDS is unable to detect elements having an atomic weight below 12. Moreover, its purpose is to provide only qualitative analysis and usually unable to provide an accurate quantitative measurement.

The TGA results come in the manifestation of two thermal curves, the TG and the DTA. The TG curve records the change of mass of the sample with respect to the gradual increment of temperature. The DTA displays the differentiation of endothermic or exothermic events occurring at the sample with respect to a thermal inert. This information gives a clue to events of the sample that may or may not have associated weight loss such as melting and crystallization or thermal decomposition. For urinary calculi, it was established by Kaloustian et al. [14, 15] that major components would consist of calcium oxalate (COM or COD), UA or magnesium ammonium phosphate hexahydrate (MAPH). Each of these major components has their unique DTA or TG signature that identifies their inclusion in the sample.

Results

The nine kidney stone samples are labeled from A to I as shown in Fig. 1. They are labeled in accordance to their major compositions after they are analyzed by both the TGA and EDS tests. Below are the derivation examples of sample composition by means of TG and EDS. The examples cover the three major main compositions that have been found in the samples. These are UA, calcium oxalates and MAPH. The nine kidney stone samples could be categorized into the following groups.

Uric acid: samples A, B.
Calcium oxalates: samples C, D, E, F.
MAPH: samples G, H, I.

Uric acid

Sample A is chosen as an example of UA for the derivation of its chemical composition. UA has fairly homogeneous microstructure. Concentric laminar rings can be frequently observed in UA samples. Sample A is brown colored with dimensions of $5.9 \times 5.7 \times 3.2$ mm. Its cross-section reveals concentric laminar layers (Fig. 2).

Sample A displays the TGA curve shown in Fig. 3. The DTA endothermic peak at $T = 450$°C corresponds to UA decomposition, The TG terminal weight loss of almost 100% supports the postulation that sample A consists of mostly UA. The mini endothermic peak at $T = 325$°C could be due to the presence of organic content like blood or protein. EDS tests are conducted at different regions around the sample and shows consistent EDS results. The EDS shows elemental peaks of C, N, and O only (Fig. 4). This further supports the conclusion that sample A consists of UA. Sample B which consists of UA also shows similar lamellar structure (Fig. 5).

Calcium oxalate

Sample C is chosen as an example of calcium oxalate for the derivation of its chemical composition. Calcium oxalate samples usually display distinct and concentric laminar layers about a nuclei. Specimen C is a sample with brown exterior and a globular structure with dimensions $8.1 \times 4.5 \times 4.7$ mm. There are two distinct regions. One is at the internal structure which consists of the globular and laminar microstructure. The other is the white powdery substance that seems to attach itself to the external surface of the sample (Fig. 1). In the case of sample C, the TG analysis (shown in Fig. 6) is focused more on the internal composition of sample C, which means that the white powdery substance is deliberately removed during the TG analysis.

Another point to note is that in the case of calcium oxalates, the water of crystallization is of interest. The hydration ratio is defined to be the number of water molecule per calcium oxalate molecule. This value is usually between 1 and 2. This is because calcium oxalate crystals in nature exist in the form of calcium oxalate monohydrate (COM, $CaC_2O_4{\cdot}H_20$) or calcium oxalate dihydrate (COD, $CaC_2O_4{\cdot}2H_20$). Calcium oxalate stones are usually composed of both forms in mixed quantities.

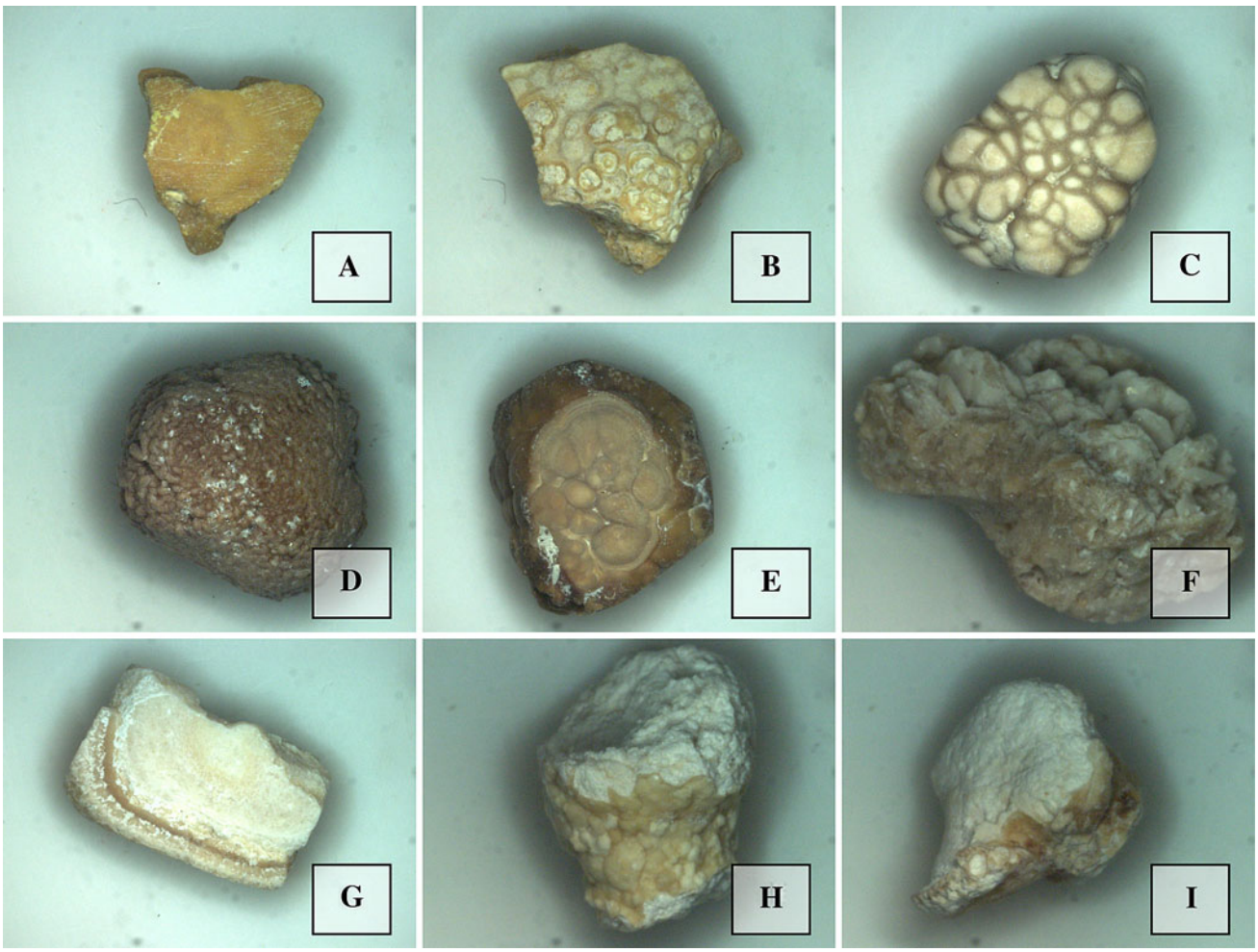

Fig. 1 The microscopic pictures of the nine kidney stone samples

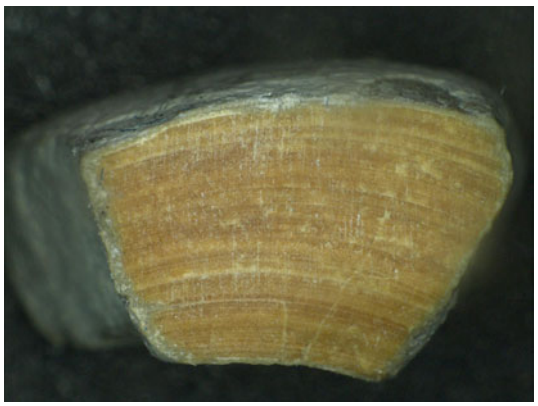

Fig. 2 Microstructure of sample A

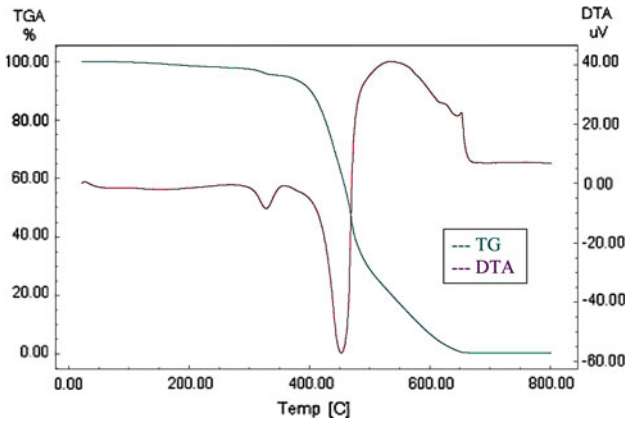

Fig. 3 TG–DTA analysis of sample A

Comparing with reported thermogravimetric data [13], the three major steps of weight loss at 200, 440 and 740°C corresponds to calcium oxalate decomposition. We observed water mass loss of 12% at the first step and a 26% mass loss of carbon dioxide at the third step.

$$[H_20]/[CO_2] = (12/18)/(26/44) = 1.1282.$$

This places the hydration ratio at 1.13. Terminal weight loss stands at 60%. The theoretical weight loss of calcium oxalate at which the hydration ratio is 1.13 is 62.1%. Thus,

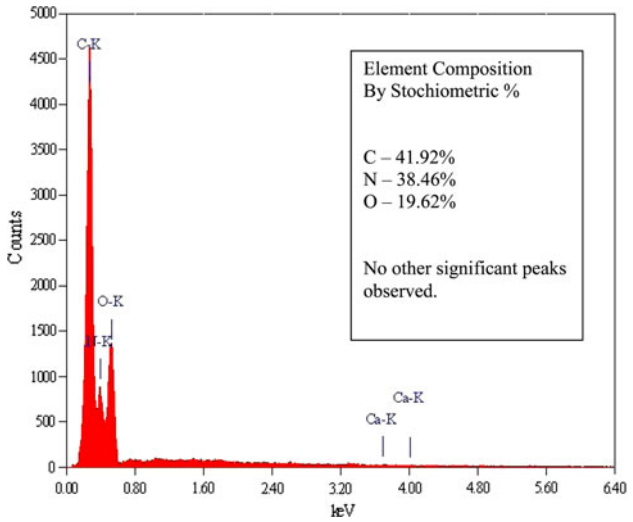

Fig. 4 EDS results for sample A

Fig. 5 Lamellar microstructure of sample B

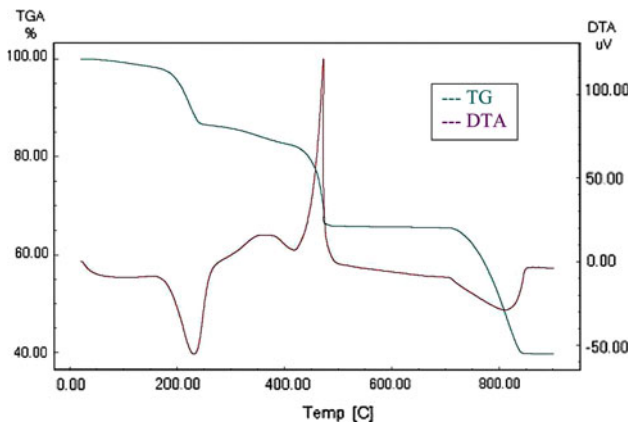

Fig. 6 TG–DTA analysis of sample C

the percentage composition of calcium oxalate stands at 96.5%.

EDS is carried out at both the laminar and white powdery regions so that there is an appreciation of the different chemical compositions. Within the laminar microstructure, multiple EDS analyses have been carried out and EDS does not show any significant difference in elemental composition even though there is a visual difference in microstructure.

The internal composition seems to consist of mainly Ca, C and O (Fig. 7). The trace amount of P is probably due to contamination that comes from white powdery substance. We can observe a surge of phosphorus (P) at the white region (Fig. 8) compared to those at the laminar region. This we can attribute to calcium phosphate, of which when subjected to heat treatment, is resistant to decomposition. The white powdery substance on the exterior must have been calcium phosphate. Sample C is a good example for the combinational application of both TGA and EDS for the characterization of the chemical compositions.

Magnesium ammonium phosphate hexahydrate

Sample G is chosen as an example of MAPH for the derivation of its chemical composition. In this particular sample, there is distinctly a thick opaque brown external layer surrounding the white internal region. This observation is of analytical interest. The white region seems to be composed of white crystals of various sizes randomly distributed about the white substance surrounding it. Specimen G measures 8.8 × 6.8 × 3 mm. For the TGA analysis, the internal white substance is tested for its contents. EDS is performed at both the internal region and the external region.

The TG curve as shown in Fig. 9 is a classical case to indicate the presence of MAPH in the interior of the sample. The endothermic peak at 160°C and the almost immediate decomposition at the beginning of the thermal treatment are indicative of MAPH presence. The terminal weight loss of pure MAPH is theoretically at 54.7%. The

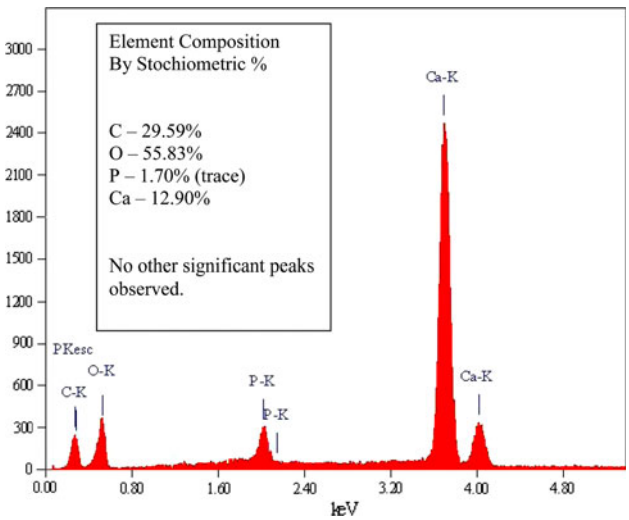

Fig. 7 EDS of laminar region of sample C

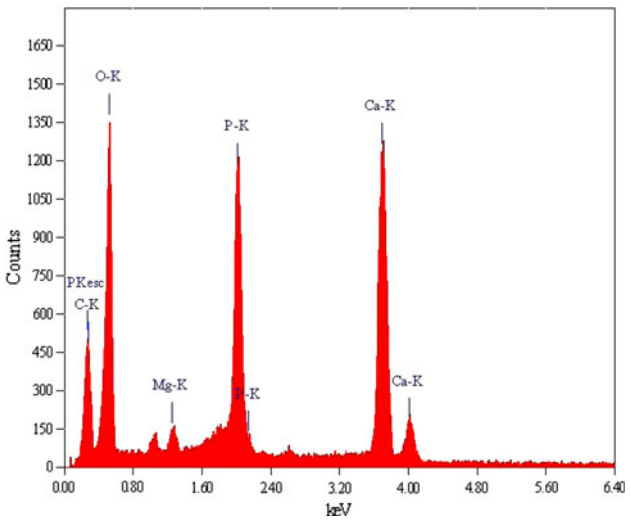

Fig. 8 EDS of white powdery region of sample C

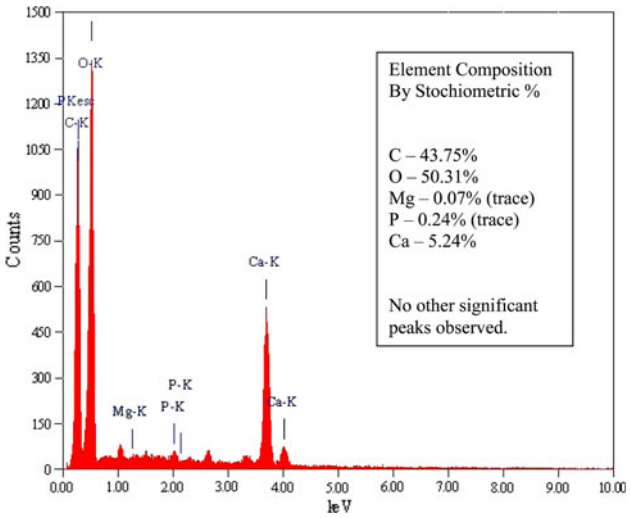

Fig. 10 EDS of sample G, exterior

TG data shows 35% weight loss. Due to the minimal disruption to the DTA curve, we can postulate that calcium phosphate is the secondary component. This is because it is resistant to thermal decomposition. From calculations, $35/54.7 = 0.639$.

Since there are two distinct regions, EDS is carried out at both regions so that there is an appreciation of the different chemical compositions. The EDS of the exterior (Fig. 10) reveals the elements C, O and Ca. There are also traces of P and Mg present but there are not of significant content. The EDS is characteristically similar to those of calcium oxalate.

The EDS of the white interior (Fig. 11) shows a significant difference in detection of phosphorus and magnesium at the white region compared to those at the exterior. The result points to the presence of MAPH in the interior, as well as suggests that the exterior is made of calcium oxalate, due to the apparent lack of magnesium and phosphorus peaks. From the TG graphs, the lack of DTA disruption

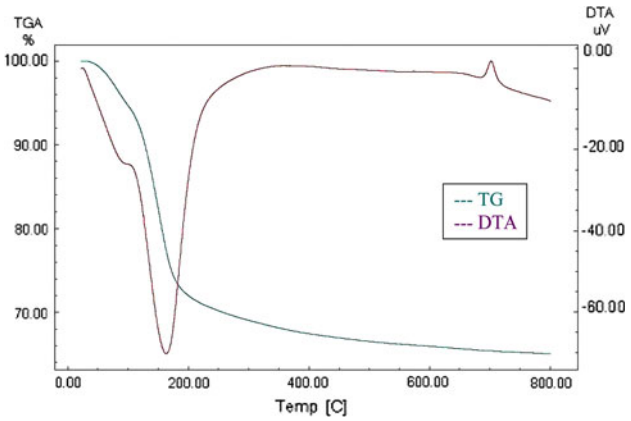

Fig. 9 TG–DTA analysis of sample G

suggests that calcium phosphate is the secondary component in the interior. Specimen G is composed of about 64% MAPH/36% calcium apatite internally and the exterior is made of calcium oxalate. Sample G is also a good example for the combinational application of both TGA and EDS for the characterization of the chemical compositions.

Hardness

The hardness values of the various samples are computed using the microhardness test and the equation,

$$\mathrm{HV} = 1{,}854\ P/d^2.$$

Of which HV is in kg/mm^2, d (the average diagonal length of a Vickers indentation in mm) and P is the load (kg).

Some kidney stone samples display regional differences in microstructures and for those samples, the microhardness of each distinct region is tested. Five hardness readings were taken for each region and the average is recorded.

Table 1 shows the calculated chemical compositions of each sample together with their average HV readings. For calcium oxalates, their hydration ratios are included as well. The values are comparable to the reported range of values by Zhong et al. [2] and Heimbach et al. [16].

Discussion

Uric acid: samples A and B

Both samples display brown cross-section with visible laminar layers. Sample A (Fig. 2) displays thin concentric laminar rings while sample B (Fig. 5) displays thick flat laminar layer. The hardness of sample A is significantly

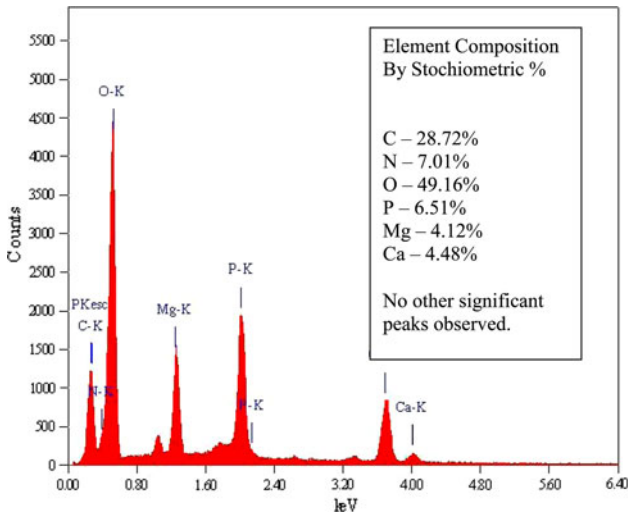

Fig. 11 EDS of sample G, white interior

higher than sample B (52.5 vs. 32.4). This suggests that sample B is more porous than sample A. From macroscopic observation, other than the thickness of laminar boundaries, there are no other notable differences.

Calcium oxalates: samples C, D, E and F

For samples C, D and E, it can be observed that the outer surface displays a reddish-brown color. Another common similarity would be the tendency to develop a microstructure that displays laminar concentric ring(s). Their hydration ratio ranges from 1.13 to 1.22. For samples C and E, they form multiple globular structures that suggest the presence of multiple nuclei. For sample D, there appears to be only one nucleus. Hardness value of samples C and E is also observed to be superior to that of sample D (99.2 and 85.1 vs. 65.2) even though the degree of hydration is around the same value. In addition, samples C and E display homogeneity in their hardness value compared to sample D, which has two distinct HV for the exterior and inner core. There are two correlations that we can make by this observation. Firstly, multiple nuclei may suggest greater hardness in the sample. Secondly, the presence of multiple nuclei increases the degree of homogeneity in the hardness of the sample. A possible explanation is that multiple nuclei means that there are multiple points of nucleation and there will be more grain boundaries created within the microstructure that increases the hardness of the sample. The homogeneity of the hardness of sample can be explained by the fact that multiple nuclei limited the physical distance of regions away from each nucleus and thus the degree of nucleation. Therefore, it might not be that the samples are homogeneous, but it is because there is less degree of nucleation in a sample with multiple nuclei than one sample with a single nucleus. Sample D's exterior hardness value is noted to be at the lower boundary of previous studies and its inner core is quite out of the lower limit. Sample D is also interesting because its inner core shows relatively less hardness compared to the external surface. There are two possible reasons—porosity and degree of hydration. As can be observed from the microstructure, there are hollow spaces in the inner core of sample D that suggest a high degree of porosity at the core. This observation can explain the relative softness of the core. Secondly, when EDS is carried out on both inner core and external surface, the inner core displayed less degree of hydration. Perhaps the degree of hydration also affects the relative hardness of calcium oxalates.

Sample F

Sample F is macroscopically different from samples C, D and E. Even though the chemical composition is predominantly calcium oxalate, its exterior boasts sharp crystals

Table 1 The composition and hardness values of the kidney stone samples

No.	Percentage of compositions	Regional difference	Hardness value(s) (kg/mm^2)		Hydration ratio
Uric acid (UA)					
A	UA (100)	Not observable	52.5	–	–
B	UA (100)	Not observable	32.4	–	–
Calcium oxalates (COM/COD)					
C	CO/MAPH (96.5/3.5)	Yes	99.2 (globular)	50.5 (white region)	1.13
D	CO (100)	Yes	65.2 (outer layer)	49.0 (inner core)	1.18
E	CO/CA (96/4)	Not observable	84.2		1.22
F	CO/CA (79/21)	Not observable	85.1	–	1.44
Magnesium ammonium phosphate hexahydrate (MAPH)					
G	MAPH/CA (64/36)	Yes	65.5 (exterior)	25.5 (interior)	–
H	MAPH/CA (70/30)	Not observable	20.2	–	–
I	CA/MAPH/CO (48/30/22)	Not observable	24.7	–	–

unlike the circular smooth reddish-brown exterior that samples C, D and E display. Furthermore, the microstructure did not reveal any regularity in structure and is relatively anisotropic. Its average hardness value is around 84.2 and is consistent with reported studies. The notable difference is the substantial increase of hydration ratio over the other samples as well as the increase in calcium apatite content. It is often quoted that COD tends to form sharp-edged crystals while COM forms smooth round kidney stones. This study's result is consistent with that general observation.

MAPH: samples G, H and I

MAPH usually come in the form of a white powdery substance. Sample G, H and I have very similar hardness value in the range of 20–25, which is about the hardness value cited in previous studies. Although the range of calcium apatite content varies, the hardness value did not fluctuate too much. From the observation of sample content, it appears that MAPH is frequently found together with calcium oxalate and calcium apatite. The brown substance found in samples H and I suggest the presence of calcium oxalate. MAPH is known to form due to urinary tract infection.

Conclusion

The samples are found to be UA, calcium oxalates and MAPH. TGA is indeed a viable analytical tools for kidney stones as it is fast and simple. While other coupled methods like FTIR and XRD are already widely used, they may at times only provide an aggregated result of the kidney stone sample. Therefore, the recommendation of EDS is practical when there is a need for differentiated qualitative chemical composition detection at the identified nuclei position for urinary calculi with spatial variation in composition. EDS can provide the rapid and simple qualitative analysis required. This facilitates the correct diagnosis and treatment by clinicians. EDS is also applicable when elemental comparison need to be made within a single sample. For example, the degree of hydration can be compared by the intensity of oxygen band.

As with TG and other form of analysis, the disruption from organic contents like blood and protein could tamper with the accuracy of the results. Another general issue is that calcium phosphate ($Ca_3(PO_4)_2$) does not show any peak in DTA nor any indication of weight loss by TG. In calcium oxalate samples, the presence of multiple nuclei and degree of nucleation is of great interest as it largely affects the macroscopic structure of the kidney stone as well as the hardness value. The results in general agrees with the findings that the greater the hydration ratio, the greater the tendency to form sharper crystals in the exterior. The presence of multiple nuclei seems to increase the degree of homogeneity of the samples as well as the hardness value.

It should be pointed out that the Infra imaging coupled with microanalysis will also be able to obtain the local molecular fingerprints with activity in the infrared region. The methodology presented in this paper would be an alternative approach for laboratories with existing SEM and TGA test facilities. The relative merits of these two approaches can only be ascertained with more detailed comparative studies.

Conflict of interest The authors would like to declare that there is no issue related to conflict of interest for this study.

References

1. Pak CY (1998) Kidney stones. Lancet 351:1797–1801
2. Zhong P, Chuong CJ, Goolsby RD, Preminger GM (1992) Microhardness measurements of renal calculi: regional differences and effects of microstructure. J Biomed Mater Res 26(9): 1117–1130
3. Bibilash BS, Vijay A, Fazil Marickar YM (2010) Stone composition and metabolic status. Urol Res 38:211–213
4. Rose GA, Woodfine C (1976) The thermogravimetric analysis of renal stones (in clinical practice). Br J Urol 48(6):403–412
5. Konjiki T, Sudo T, Kohyama N (1980) Mineralogical notes of apatite in urinary calculi. Calcif Tissue Int 30(1):101–107
6. D'Ascenzo G, Curini R, de Angelis G, Cardarelli E, Magri A, Miano L (1983) Renal calculi analysis. Application of thermal analytical techniques. Thermochim Acta 62(2–3):149–169
7. Materazzi S, Curini R, D'Ascenzo G, Magri AD (1995) TG-FTIR coupled analysis applied to the studies in urolithiasis: characterization of human renal calculi. Thermochim Acta 264(1–2):75–93
8. Ficai A, Andronescu E, Voicu G, Pall S (2010) Methodology of in vitro characterization of human uroliths. UPB Sci Bull Ser B 72(1):47–56
9. Anderson JC, Williams JC Jr, Evan AP, Kondon KW, Sommer AJ (2007) Analysis of urinary calculi using an infrared microspectroscopic surface reflectance imaging technique. Urol Res 35:41–48
10. Berényi M, Frang D, Légrády J (1972) Theoretical and clinical importance of the differentiation between the two types of calcium oxalate hydrate. Int Urol Nephrol 4(4):341–345
11. Zhong P, Chuong CJ, Preminger GM (1993) Characterization of fracture toughness of renal calculi using a microindentation technique. J Mater Sci Lett 12(18):1460–1462
12. Cohen NP, Whitfield HN (1993) Mechanical testing of urinary calculi. World J Urol 11(1):13–18
13. Mishima H, Yamamoto H, Sakae T (1992) Scanning electron microscopy-energy dispersive spectroscopy and X-ray diffraction analyses of human salivary stones. Scanning Microsc 6(2):487–493
14. Kaloustian J, Pauli A, Pieroni G, Portugal H (2002) The use of thermal analysis in determination of some urinary calculi of calcium oxalate. J Therm Anal Calorim 70(3):959–973
15. Kaloustian J, El-Moselhy TF, Portugal H (2003) Determination of calcium oxalate (mono- and dihydrate) in mixtures with magnesium ammonium phosphate or uric acid: the use of simultaneous thermal analysis in urinary calculi. Clin Chim Acta 334(1–2):117–129
16. Heimbach D, Munver R, Zhong P, Jacobs J, Hesse A, Müller SC (2000) Acoustic and mechanical properties of artificial stones in comparison to natural kidney stones. J Urol 164(2):537–544